Electronic Supplementary Material (ESI) for RSC Advances.

Monitoring the mechanism of formation of $[Ce(1,10\text{-phenanthroline})_2(NO_3)_3]$ by *in-situ* luminescence analysis of 5d-4f electronic transitions

Laura Ruiz Arana,[a] Patric Lindenberg,[a] Hajer Said,[a] Marvin Radke,[a] Niclas Heidenreich, [a, b] César dos Santos Cunha,[a,c] Sebastian Leubner [a] and Huayna Terraschke [a,*]

[a] Institute of Inorganic Chemistry, Christian-Albrechts-Universität zu Kiel, Max-Eyth-Straße 2, 24118 Kiel, Germany. E-mail: hterraschke@ac.uni-kiel.de.

[b] DESY Photon Science, Notkestr. 85, 22607 Hamburg, Germany.

[c] Institute of Chemistry, University of São Paulo, Av. Prof. Lineu Prestes 748, 05508-000 São Paulo-SP, Brazil.

Electronic supplementary information

Contents

1. Experimental Setups

Table 1: Different experimental conditions applied for *in-situ* monitoring the formation of $[Ce(phen)_2(NO_3)_3]$ (phen = 1,10-phenanthroline) at the University of Kiel (Setup I, experiment type **1**-**3**) and at the Deutsches Elektronen-Synchrotron (DESY) (Setup II, experiment types **4**-**5**).

Number of experiment type	**1**	**2**	**3**	**4**	**5**
Added $Ce(NO_3)_3 \cdot 6\ H_2O$ / mmol	0.69	0.69	0.69	0.69	0.69
Volume of $Ce(NO_3)_3 \cdot 6\ H_2O$ solution / mL	30	30	30	30	30
Added 1,10-phenanthroline / mmol	1.38	1.38	1.38	1.38	1.38
Volume of 1,10- phenanthroline solution / mL	5	5	5	5	5
Temperature / °C	35	20	25	25	30
Excitation wavelength / nm	-	400	400	-	365
Emission wavelength / nm	-	700	700	-	-
Beamline	-	-	-	P07	P09
Energy of synchrotron X-ray beam / keV	-	-	-	87.1	23

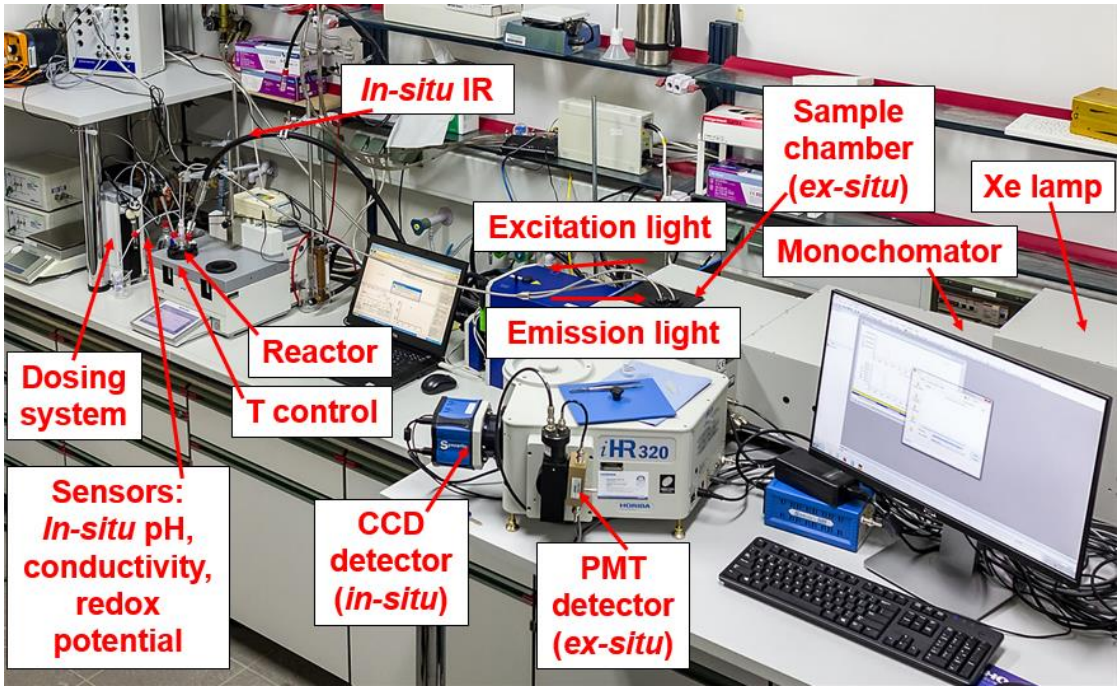

Figure S1: Setup I of the *in-situ* crystallization cell at University of Kiel showing the combination of a Mettler Toledo Easy Max™ reactor system with a Horiba Fluorolg-3 fluorescence spectrometer. The Easy Max™ reactor system includes a dosing system, temperature control, *in-situ* measurements of pH value, ion conductivity, redox potential and infrared (IR)

spectroscopy. The Fluorolg-3 fluorescence spectrometer is equipped with a Y-shaped optical fiber, a Xenon lamp, a charged-coupled-device (CCD)-based and a photomultiplier tube (PMT) detector.

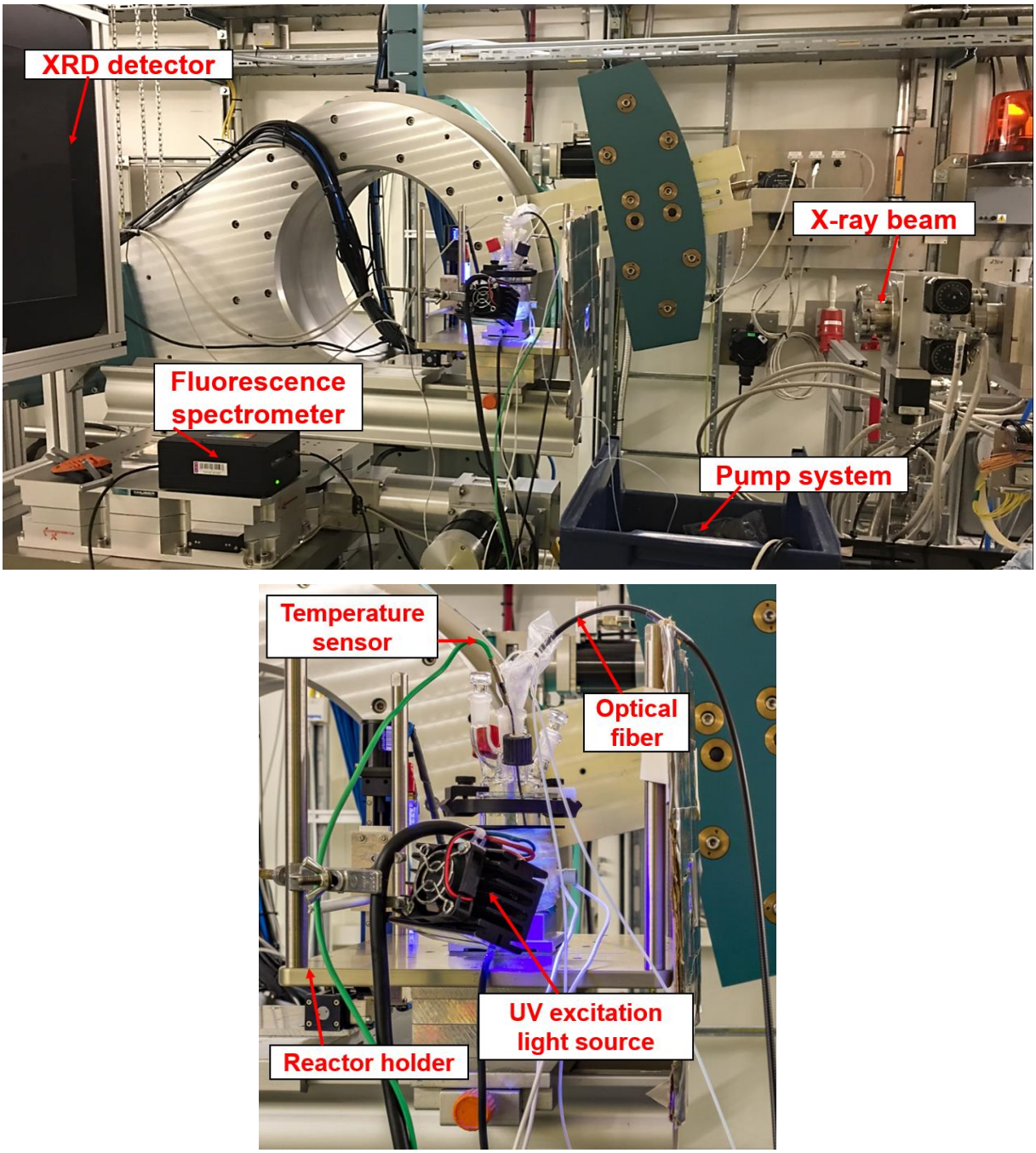

Figure S2: Setup II used at the DESY for simultaneous measurements of *in-situ* X-ray diffraction (XRD) analysis and light transmission.

2. *Ex-situ* and *in-situ* luminescence spectra

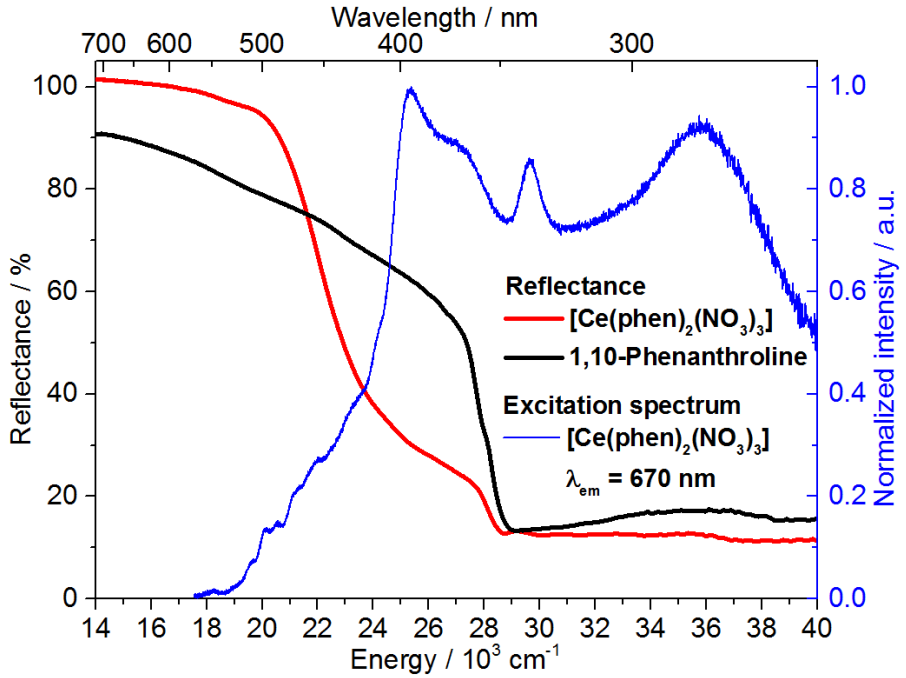

Figure S3: *Ex-situ* excitation spectrum of the $[Ce(phen)_2(NO_3)_3]$ complex (λ_{em} = 670 nm, blue curve, experiment 1, Table S1) in comparison to reflectance spectra of $[Ce(phen)_2(NO_3)_3]$ (red curve, experiment 2, Table S1) and pure 1,10-phenanthroline (black curve).

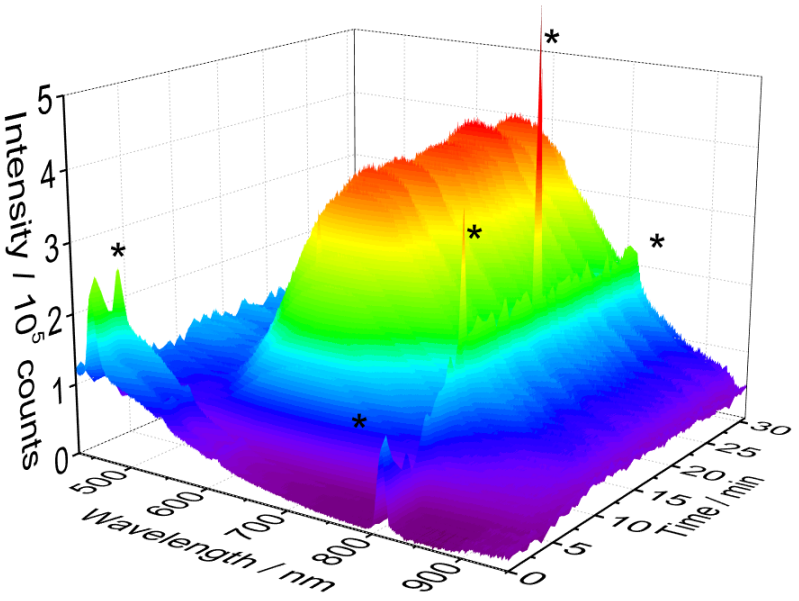

Figure S4: *In-situ* luminescence spectra (λ_{ex} = 400 nm) showing the shift of the emission band assigned to Ce^{3+} in the ethanolic solution at 415-700 nm to 500-900 nm, assigned to Ce^{3+} within the $[Ce(phen)_2(NO_3)_3]$ for monitoring the formation of the solid complex (experiment 1, Table S1). The asterisk (*) marks measurement artefacts.

3. *Ex-situ* X-ray diffraction analysis

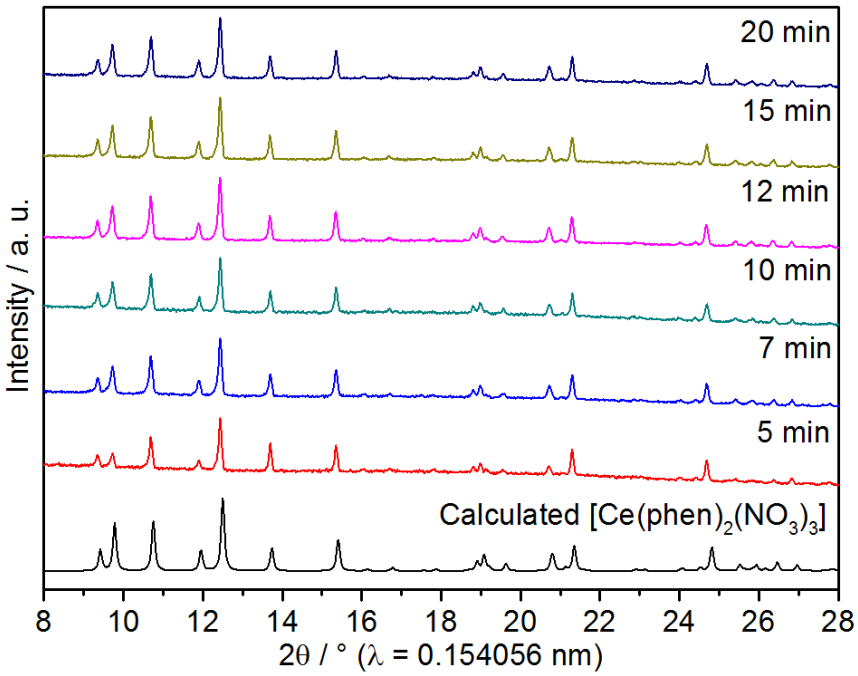

Figure S5: *Ex-situ* XRD analysis of samples removed from the reactor at t = 5, 7, 10, 12, 15 and 15 min during the synthesis of $[Ce(phen)_2(NO_3)_3]$, in comparison to the respective calculated powder pattern[1] (experiment 2, Table S1).

4. In-situ IR measurements

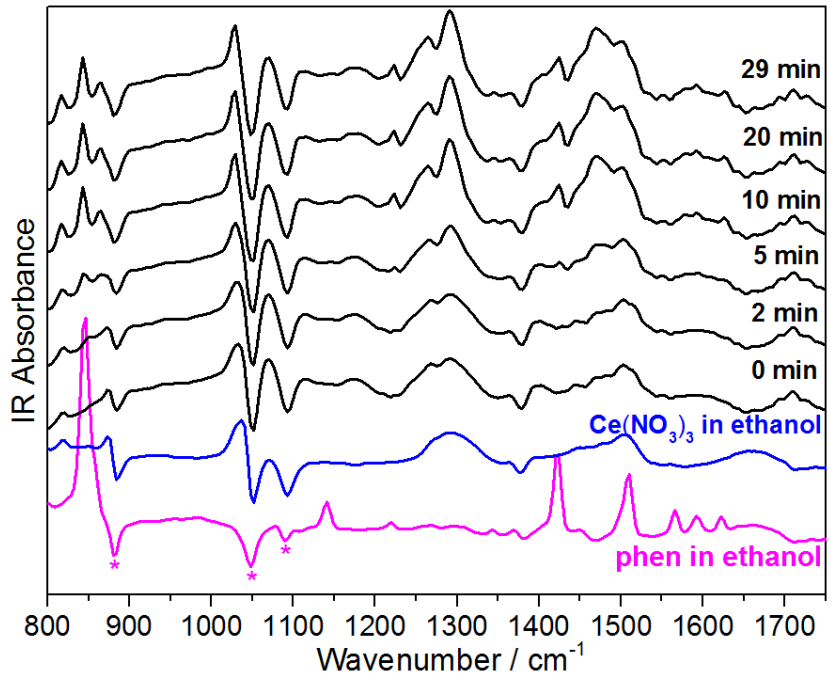

Figure S6: Infrared spectra of the initial phen and $Ce(NO_3)_3 \cdot 6H_2O$ ethanolic solutions compared to the *in-situ* IR data recorded during synthesis of $[Ce(phen)_2(NO_3)_3]$ (experiment 3, Table S1). The asterisk (*) signs show negative values for the IR bands, caused by air bubbles on the sensor.

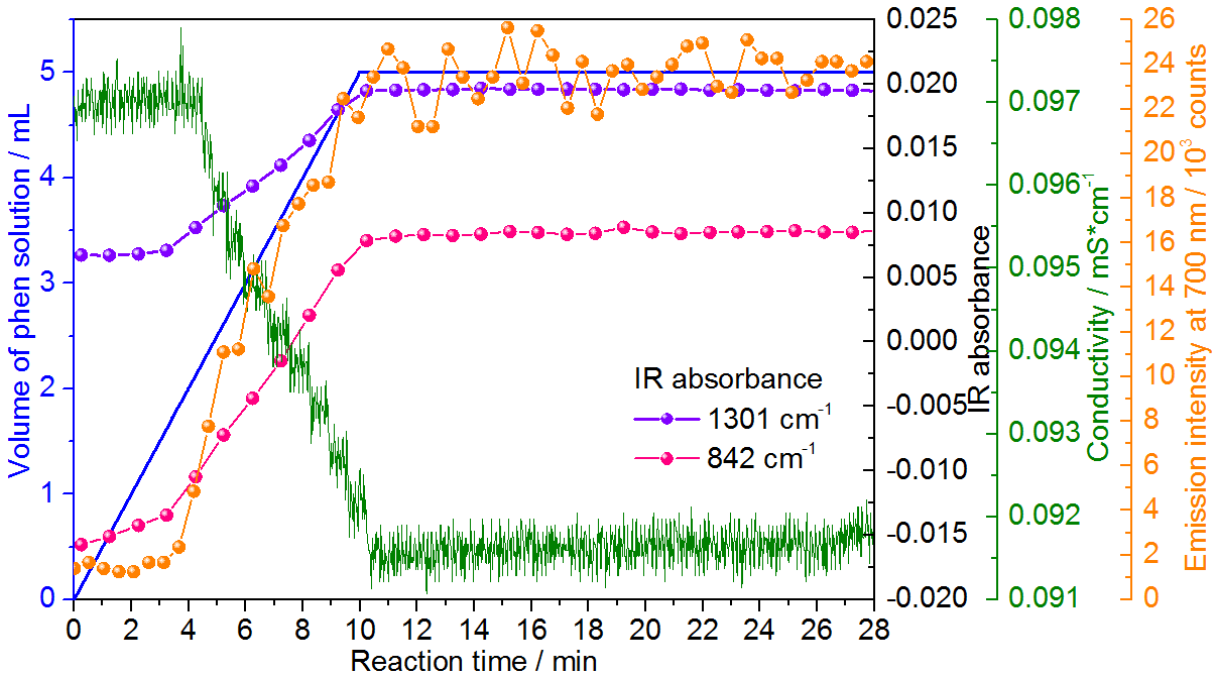

Figure S7: Time dependence of the addition of the phen solution to the $Ce(NO_3)_3 \cdot 6H_2O$ solution (blue curve), of the IR bands at 1301 cm^{-1} (NO_3^-, violet curve) and 842 cm^{-1} (phen, pink curve), of the ion conductivity (green curve) as well as of the simultaneously measured emission intensity of $[Ce(phen)_2(NO_3)_3]$ at 700 nm (orange curve) (experiment 3, Table S1).

5. *In-situ* X-ray diffraction analysis at the DESY beamline P07B

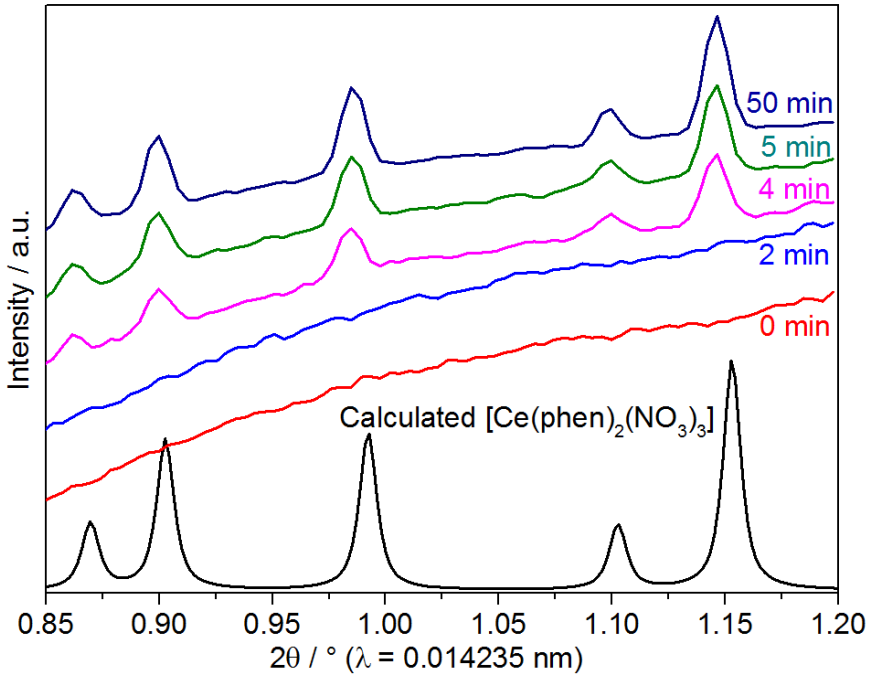

Figure S8: Time-resolved *in-situ* XRD patterns measured at the DESY beamline P07B during the formation of $[Ce(phen)_2(NO_3)_3]$ (experiment 4, Table S1) in comparison to the respective calculated pattern[1].

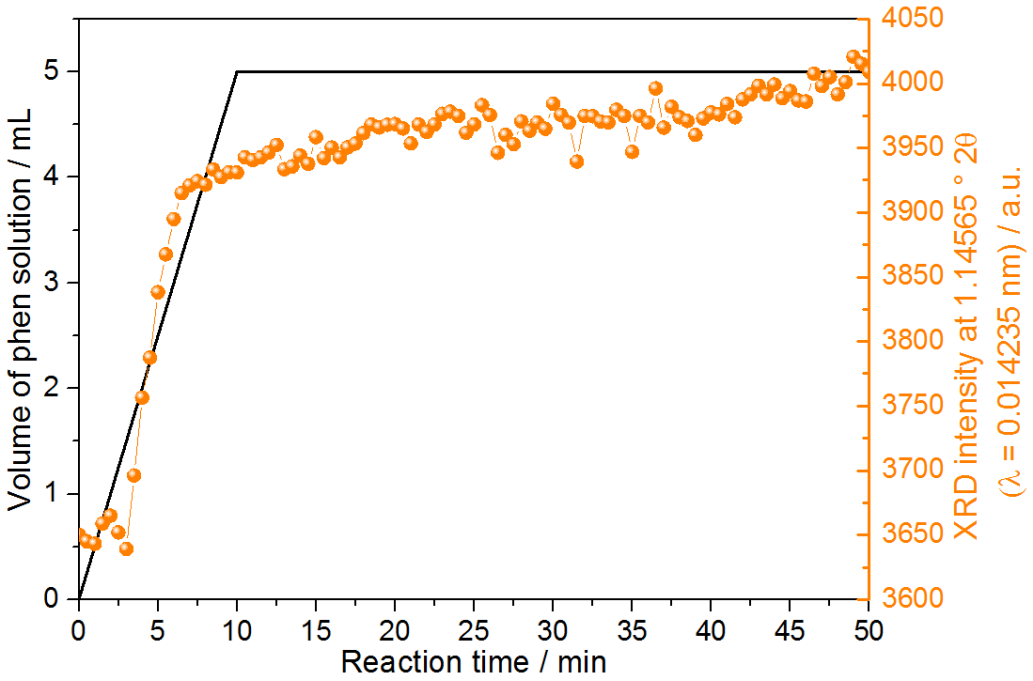

Figure S9: XRD intensity at 1.14565 ° 2θ, assigned to the (1,1,1) reflection of $[Ce(phen)_2(NO_3)_3]$ (orange curve) and time-dependence of the volume of phen solution added to the $Ce(NO_3)_3 \cdot 6H_2O$ solution (black curve) during synthesis of $[Ce(phen)_2(NO_3)_3]$ at the DESY beamline P07B (experiment 4, Table S1).

6. *In-situ* measurements of light transmission and *in-situ* X-ray diffraction analysis at the DESY beamline P09

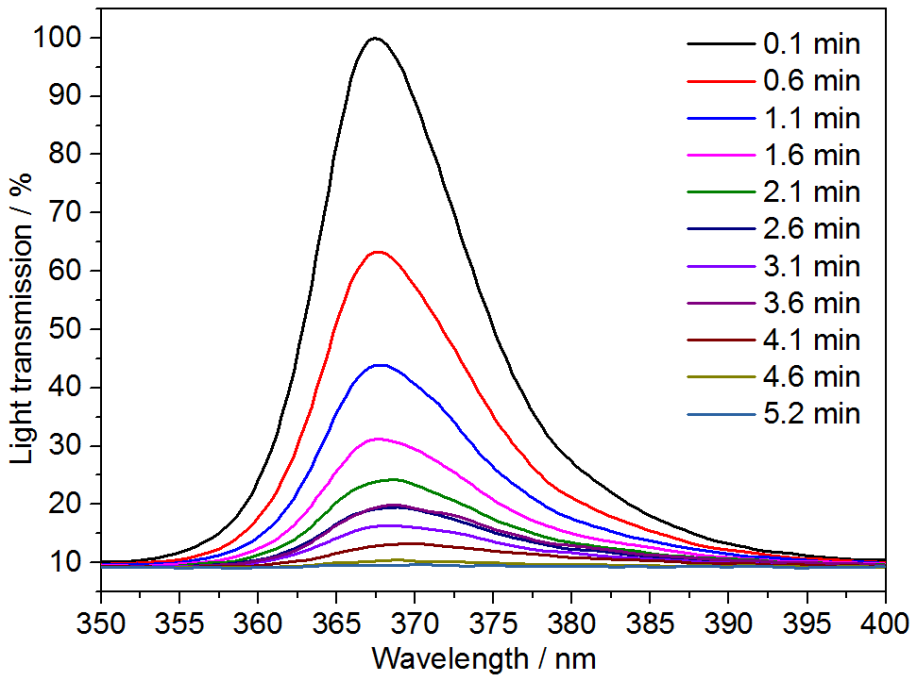

Figure S10: Time-dependent *in-situ* light transmission measured simultaneously to *in-situ* XRD at the DESY beamline P09 during synthesis of $[Ce(phen)_2(NO_3)_3]$ (experiment 5, Table S1).

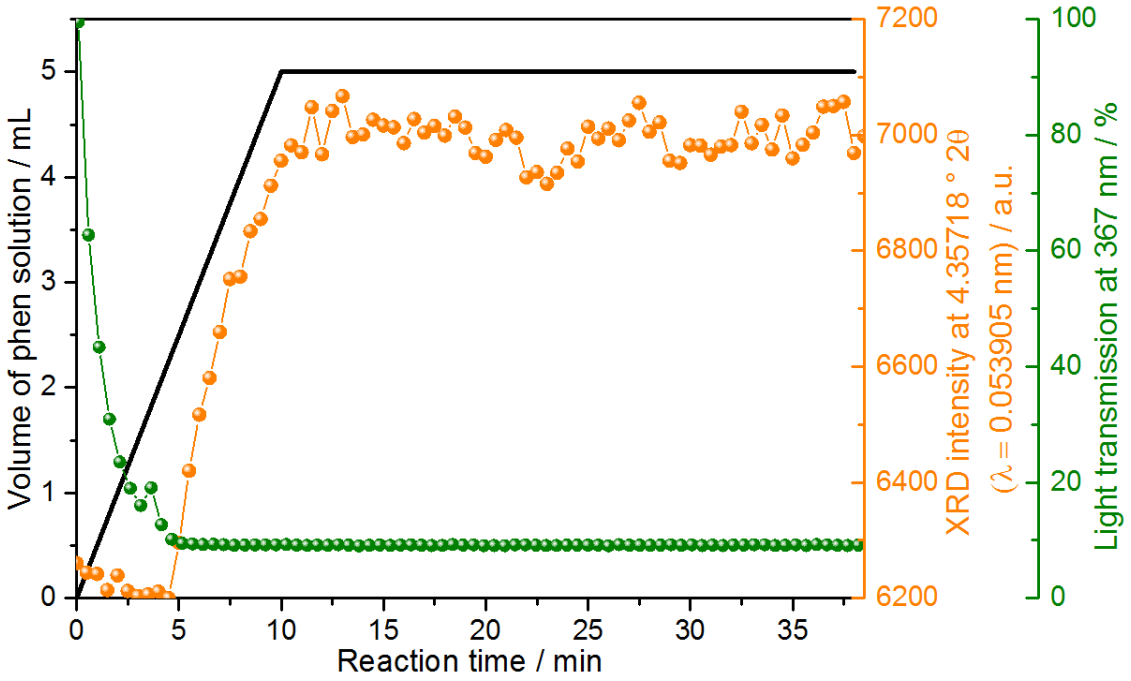

Figure S11: XRD intensity at 4.35718 ° 2θ, assigned to the (1,1,1) reflection of $[Ce(phen)_2(NO_3)_3]$ (orange curve) in comparison to the time-dependent volume of phen solution added to the $Ce(NO_3)_3 \cdot 6H_2O$ solution (black curve) and light transmission at 367 nm (green curve) during synthesis of $[Ce(phen)_2(NO_3)_3]$ at the DESY beamline P09 (experiment 5, Table S1).

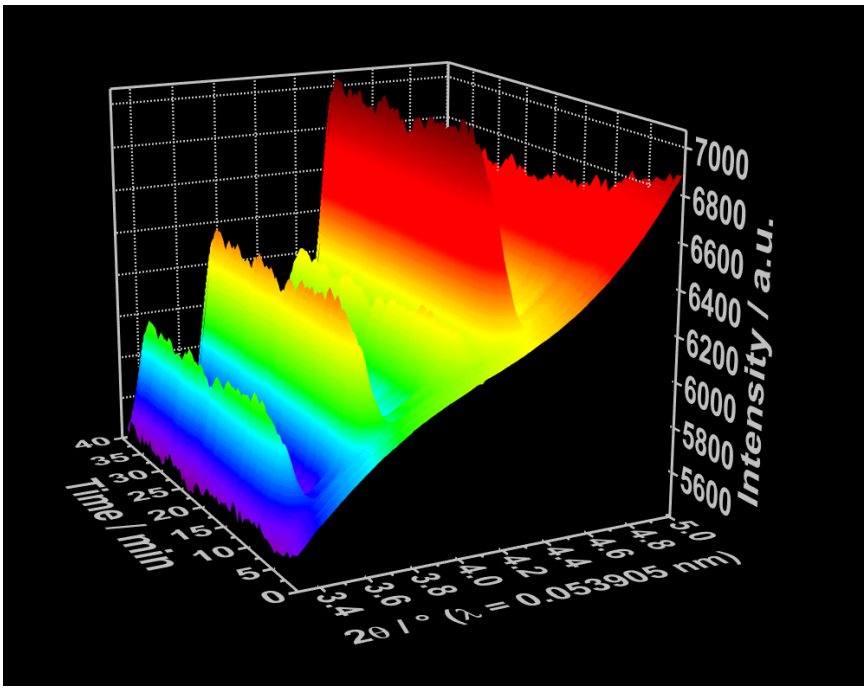

Figure S12: *In-situ* X-ray diffraction patterns measured during synthesis of $[Ce(phen)_2(NO_3)_3]$ at the DESY beamline P09 (experiment 5, Table S1).

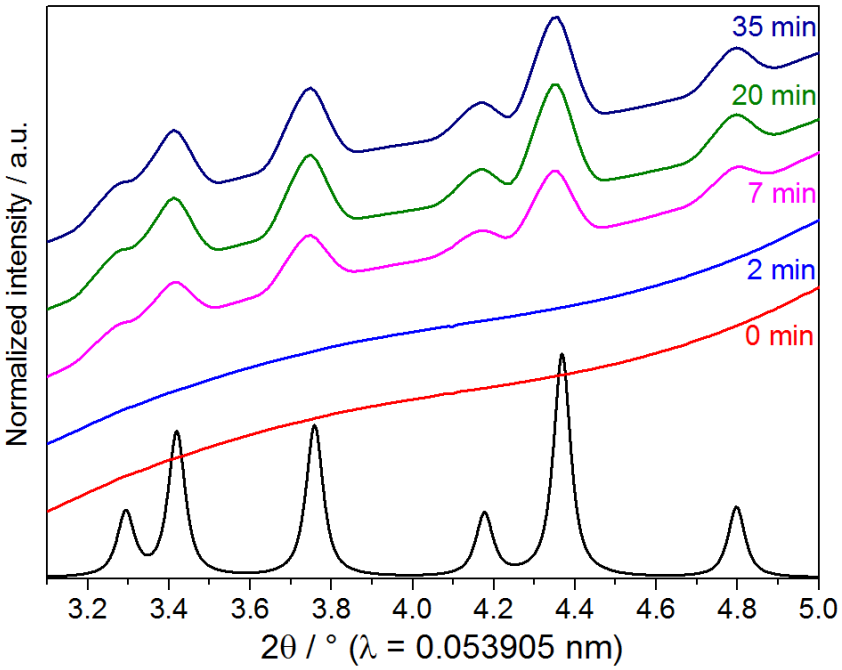

Figure S13: Time-resolved *in-situ* XRD patterns measured at the DESY beamline P09 during the formation of $[Ce(phen)_2(NO_3)_3]$ (experiment 5, Table S1) in comparison to the respective calculated pattern[1].

References

[1] Q. Y. Lin, Y. L. Feng, *Z. Kristallogr*., 2003, **218**, 531